



# Ketogenic diet compromises vertebral microstructure and biomechanical characteristics in mice

Xiuhua Wu<sup>1</sup> · Jianyang Ding<sup>1</sup> · Xiaolin Xu<sup>1</sup> · Xiaomeng Wang<sup>2</sup> · Junhao Liu<sup>1</sup> · Jie Jiang<sup>3</sup> · Qi Liu<sup>1</sup> · Ganggang Kong<sup>1</sup> · Zucheng Huang<sup>1</sup> · Zhou Yang<sup>1</sup> · Qingan Zhu<sup>1</sup>

Received: 31 July 2018 / Accepted: 19 March 2019 / Published online: 9 April 2019  
© Springer Japan KK, part of Springer Nature 2019

## Abstract

Ketogenic diet (KD) compromised the microstructure of cancellous bone and the mechanical property in the appendicular bone of mice, while the effects of KD on the axial bone have not been reported. This study aimed to compare the changes in the microstructure and mechanical properties of the forth lumbar (L4) vertebra in KD and ovariectomized (OVX) mice. Forty eight-week-old female C57BL/6J mice were assigned into four groups: SD (standard diet) + Sham, SD + OVX, KD + Sham, and KD + OVX groups. L4 vertebra was scanned by micro-CT to examine the microstructure of cancellous bone, after which simulative compression tests were performed using finite element (FE) analysis. Vertebral compressive test and histological staining of the L4 and L5 vertebrae were performed to observe the biomechanical and histomorphologic changes. The KD + Sham and SD + OVX exhibited a remarkable declination in the parameters of cancellous bone compared with the SD + Sham group, while KD + OVX demonstrated the most serious bone loss in the four groups. The stiffness was significantly higher in the SD + Sham group than the other three groups, but no difference was found between the remaining groups. The trabecular parameters were significantly correlated with the stiffness. Meanwhile, the OVX + Sham and KD + OVX groups showed a significant decrease in the failure load of compressive test, while there was no difference between the KD + Sham and SD + Sham groups. These findings suggest that KD may compromise the vertebral microstructure and compressive stiffness to a similar level as OVX did, indicating adverse effects of KD on the axial bone of the mice.

**Keywords** Ketogenic diet · Lumbar vertebrae · Microstructure · Cancellous bone · Compressive stiffness

## Introduction

Ketogenic diet (KD) is a dietary regimen with high fat, low carbohydrate, and adequate protein. The classic KD is the ratio of fat (in grams) to carbohydrate plus protein, which is nearly 4:1 (generally, but 3:1, 2:1, and even 1:1 are also

possible) [1]. Daily energy intake is restricted to 80–90% of the recommended values [2]. As a special high-fat diet, KD is used to treat diseases by switching the fuel resource from glycometabolism to lipid metabolism [3, 4].

Clinically, KD was discovered in the early 1920s for the treatment of epilepsy. Recently, it has been shown to be effective in animal models with neurodegenerative diseases, such as amyotrophic lateral sclerosis, Alzheimer's disease, and traumatic brain injury [5–9]. Although KD was regarded as a special diet therapy in the past decades, the osteoporotic influence has been attracted to the attention of the people. Some clinical studies reported that KD resulted in calcium and bone mass deficiency [10] and long-term KD induced vitamin D insufficiency [11], aggravating bone loss in children with low body mass index (BMI) [12]. There is a raising tendency regarding the use of KD, and hence it is of great importance to consider the adverse effects of KD on bones.

---

Xiuhua Wu and Jianyang Ding contributed equally to this work and should be considered co-first authors.

✉ Qingan Zhu  
qinganzhu@gmail.com

<sup>1</sup> Department of Spinal Surgery, Nanfang Hospital, Southern Medical University, 1838 North Guangzhou Avenue, Guangzhou, China

<sup>2</sup> Department of Spinal Surgery, LongYan First Hospital, Longyan, Fujian, China

<sup>3</sup> Department of Spinal Surgery, Hongdu Hospital of TCM, Nanchang, Jiangxi, China

In fact, osteoporosis is a skeletal disease in which the bone mass declines and the trabecular architecture deteriorates, leading to increased bone fragility and risks of spontaneous fractures [13, 14]. This has become a serious health problem as it predisposes patients to fragility fractures [15]. Osteoporotic fractures usually occur at sites with relatively high proportion of trabecular bone, such as proximal femurs, distal radius, and vertebral bodies [16]. Among these, vertebral fracture is one of the most common clinical manifestations that occur due to osteoporosis under non-traumatic events [17]. According to our previous research, KD compromised the microstructure of cancellous and cortical bone in the femur of C57 female mice [18], while many other studies demonstrated that the bone mass changes the axial as well as appendicular bones, concluding that the changes of the bone structure in different parts were not exactly the same [19]. The effects of KD on vertebrae microstructure and biomechanical properties in animals have not been reported yet. The present study was aimed to verify the osteoporotic effects of KD on vertebral body in comparison to that of ovariectomy (OVX), and analyze the biomechanical properties by micro-finite element (micro-FE) simulated test and vertebral compressive test.

## Materials and methods

### Experimental ethics

This study was approved by the Animal Experiments Ethics Committee of Southern Medical University. Forty healthy female C57BL/6J mice aged 6 weeks were purchased from the Laboratory Animals Center of Southern Medical University. The whole experiment was performed according to the Guidelines of Caring for Laboratory Animals by the Ministry of Science and Technology of the People's Republic of China.

### Animal husbandry

All mice (eight-week-old, female) had free access to water and a standard laboratory rodent diet for 2 weeks to ensure acclimatization, and then were randomly divided into two main groups, i.e., SD (standard diet) group and KD (ketogenic diet) group. The SD group was then subdivided into SD + Sham (SD + ovary intact) group and SD + OVX (SD + ovariectomy) group, and the KD group was assigned into KD + Sham (KD + ovary intact) group and KD + OVX (KD + ovariectomy) group. For ovariectomized mice, the bilateral ovaries were identified and removed under anesthesia using isoflurane. All mice were individually placed in plexiglass ventilated cages in a controlled environment ( $21.3 \pm 0.6$  °C) and maintained on a 12-h light–dark cycle.

All mice had free access to diets and tap water during the entire experimental period. The mice in the SD groups were fed with a normal diet (provided by Laboratory Animals Center of Southern Medical University, Table 1). The mice in the KD groups were fed with a ketogenic diet with a ratio of fat to carbohydrate + protein of 4:1 (Ketogenic Cookies, Zeneca, Shenzhen, China, Table 1), which has been used in the clinical treatment of epilepsy.

### Body and uterus weight, blood ketone and glucose measurement

The uterus with oviducts was carefully excised from the adherent tissues, fixed in normal saline individually, and stored at 4 °C for weight measurement by analytical balance (Mettler Toledo Scale, Switzerland). Body weights of all mice were measured every 2 weeks for 12 weeks using a CS 200 scales (Ohaus, Pine Brook, NJ, USA).

Blood samples were obtained by cutting the tail veins. Blood glucose and ketone levels of the mice were tested for each fortnight from 8 to 20 weeks of age, with two samples measured in each turn. The blood glucose level was tested using monitor JPS-5 (Leapon Inc., China) and blood  $\beta$ -hydroxybutyrate level was measured by Yicheng Blood Ketone Meter T-1 (Sentest Inc., China) and Medisense Precision Xtra monitor (Abbott Laboratories, Canada).

### Micro-computed tomography scan

Twenty-week-old mice were euthanized under anesthesia using isoflurane. The lumbar vertebrae were separated, the soft tissue was cleaned, and then fixed in 4% paraformaldehyde for 24 h. After that, the lumbar vertebrae were transferred to 75% alcohol, and then stored at 4 °C environment until scanning.

**Table 1** Basic nutrient content comparison between standard and the ketogenic diet

Projected(per 100 g)	Standard diet	Ketogenic diet
Energy	1338 kJ	1748 kJ
Protein	14.5 g	6.1 g
Fat	4 g	37.1 g
Carbohydrates	55.5 g	3.1 g
Dietary fiber	4.5 g	27.5 g
Sodium	130 mg	144 mg
Calcium	720 mg	117 mg
Phosphorus	600 mg	81 mg
Vitamin D	2.5ug	0.03ug

The weight ratio of fat to carbohydrate + protein in ketogenic diet is 4: 1

The lumbar vertebrae were fixed in a cylindrical plastic tube to prevent movement during scanning by micro-computed tomography (micro-CT) ( $\mu$ CT 80, Scanco Medical AG, Bassersdorf, Switzerland). The fourth lumbar vertebra (L4) was scanned at anisotropic voxel size of 12  $\mu$ m (55 kv, 145  $\mu$ A, integration time 300 ms, averaged two times). The gray-scan images were processed using a low-pass Gaussian filter ( $\sigma = 0.8$ , support = 1) to remove noise. A threshold of 220 was used to extract the mineralized bone from soft tissue and marrow phase. The software for analyses was provided by Scanco, and 100 slices were chosen in the middle of the vertebral body for cancellous bone analyses. Trabecular parameters included tissue mineral density (TMD), bone mineral density (BMD), bone volume/tissue volume (BV/TV), trabecular thickness (Tb.Th), trabecular number (Tb.N), trabecular separation (Tb.Sp), connectivity density (Conn.D), and structure model index (SMI).

### Micro-finite element analysis

To determine the stiffness of the vertebrae, virtual compression tests by micro-FE simulations were performed. The micro-FE software (SCANCO Medical AG, Version 1.13) in addition to the Image Processing Language (IPL) software were delivered by Scanco for image manipulation and enhancement. High-resolution three-dimensional (3D) images of the tissue were used to generate micro-FE models and to estimate the local mechanical stimuli [20]. The simulations were done within the framework of linear elasticity. The elastic material properties were supposed to be homogeneous (no distinction between cortical and trabecular bone) and isotropic with a Poisson's ratio of  $\nu = 0.3$  and Young's modulus of material =  $1 \times 10^4$  MPa. The test was conducted by "high-friction compression test in the  $z$ -direction" to simulate the compression test. The simulated biomechanical parameter was stiffness.

### Vertebral compressive test

To evaluate the mechanical properties of the vertebra, the axial compressive test was performed using a materials testing machine (Electropuls E1000, Instron Inc., MA) with a load cell of 50 N. The L4 vertebral body was tested by compression with loads applied along the craniocaudal axis. Before testing, the attachments, and the upper and the lower endplates were removed. A compressive force was applied to the vertebra at a speed of 2 mm/min. The test was automatically stopped until the bone tissue was broken. Load-deformation curves were plotted and failure load (Fmax) was analyzed.

### Histological staining

The L5 vertebra was embedded into the olefin following the decalcification in 10% EDTA for 4 weeks. After that, all the samples were disposed for iron hematoxylin–eosin staining, which was performed to observe the histomorphology of the trabecular bone.

### Statistical analysis

Data were presented as means  $\pm$  standard deviation. A 2-factor analysis of variance was used to determine the effect of diet (KD or SD) and treatment (OVX or Sham) on bone microstructure parameters, the micro-FE and compressive test data. Multiple comparisons were performed using the SNK tests. Correlation analysis was completed across all the paired samples of cancellous bone morphological and mechanical variables. For all statistical tests,  $p < 0.05$  was considered to be statistically significant.

## Results

### Measurements of uterus and body weight, blood ketone and glucose levels

Success of OVX was confirmed by a marked atrophy of the uterus (Table 2). The uterine weight of ovariectomized mice (SD + Sham group  $0.107 \pm 0.025$  g and KD + Sham group  $0.108 \pm 0.037$  g) was significantly lower compared with ovary intact mice (SD + OVX group  $0.025 \pm 0.012$  g and KD + OVX group  $0.022 \pm 0.012$  g). There was no significant difference regarding the body weight of the mice before dietary interventions in all groups (Table 2). Different diet interventions showed no significant weight changes after 12 weeks of feeding (SD groups  $23.67 \pm 2.58$  g vs KD groups  $23.75 \pm 0.5$  g,  $P < 0.05$ ) (Table 2).

Blood glucose levels between the KD groups and SD groups showed no differences during the experiment, and the average blood glucose level was similar to each other (SD groups  $11.06 \pm 1.73$  mmol/L vs KD groups  $11 \pm 1.87$  mmol/L). However, the blood ketone levels in

**Table 2** The body weight and uterine weight among groups

Group	initial bodyweight	Body weight(g)	Uterine weight(g)
SD + Sham	$19.0 \pm 1.00$	$23.7 \pm 0.577$	$0.107 \pm 0.025$
KD + Sham	$18.3 \pm 1.50$	$24.0 \pm 0.00$	$0.108 \pm 0.037$
SD + OVX	$18.0 \pm 2.64$	$22.3 \pm 1.53$	$0.025 \pm 0.012^*$
KD + OVX	$19.3 \pm 0.577$	$25.0 \pm 3.00$	$0.022 \pm 0.012^*$

Data are presented as means  $\pm$  SD. \* $P < 0.05$ , compared with SD + Sham group

the KD groups were apparently higher than that in the SD groups at all time points (SD groups  $0.37 \pm 0.26$  mmol/L vs KD groups  $0.85 \pm 0.21$  mmol/L). The daily change of animal body weight, blood glucose and ketone levels were reported in our previous study [18].

### Micro-CT results

The SD + OVX group displayed a significant decrease of BV/TV, Conn.D, Tb.N, Tb.Th and TMD, obvious increase of both SMI and Tb.Sp in the L4 vertebral trabecular parameters when compared to the SD + Sham group. Noticeably, KD deteriorated the cancellous bone in the KD + Sham

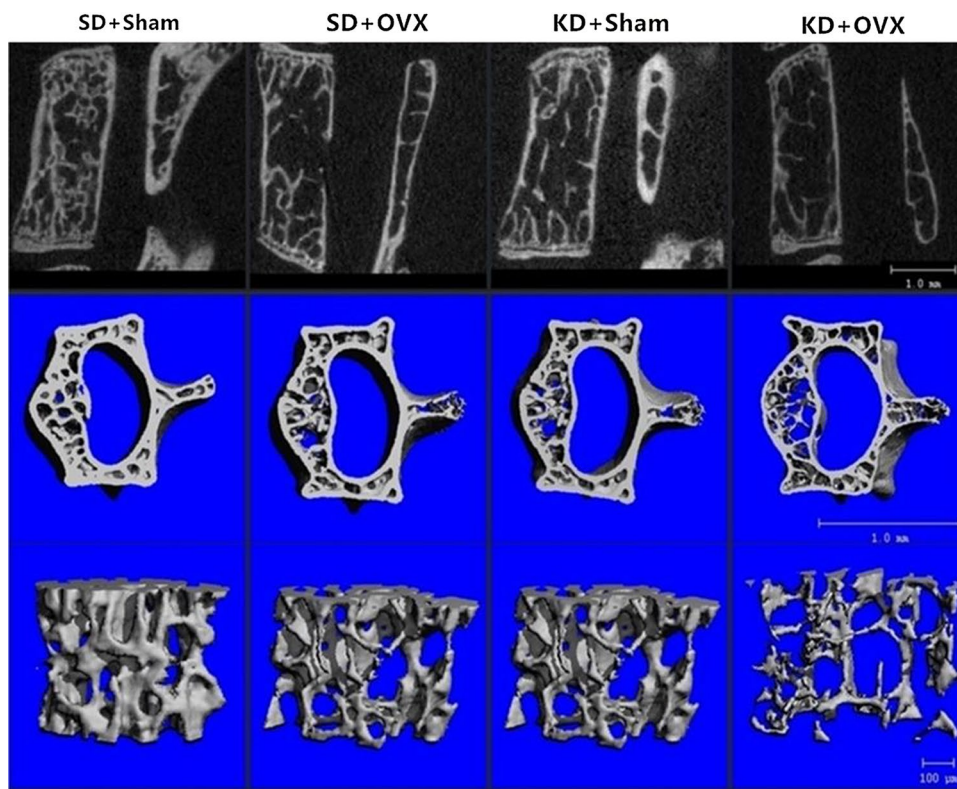
group, but the Tb.Th and Tb.Sp showed no significant changes. There were no remarkable differences in all the trabecular parameters between KD + Sham and the SD + OVX groups, except for BMD. (Table 3, Fig. 1). The KD + OVX group revealed severe cancellous bone loss in L4 vertebra compared with the other three groups. When compared to the SD + Sham group, the KD + OVX showed a significant reduction in BV/TV, Conn.D, Tb.N, Tb.Th and TMD, while an increase in SMI and Tb.Sp. The KD + OVX group also demonstrated lower Conn.D than the SD + OVX group, but higher SMI ( $P < 0.05$ ). It also had lower levels of BV/TV, Conn.D, Tb.N, TMD and BMD, but higher Tb.Sp when compared with KD + Sham group. (Table 3, Fig. 1).

**Table 3** Micro-CT analysis of cancellous bone of the L4 vertebrae at 12 weeks

Parameters	SD + Sham	SD + OVX	KD + Sham	KD + OVX
BV/TV	$0.236 \pm 0.080$	$0.147 \pm 0.036^*$	$0.162 \pm 0.024^*$	$0.107 \pm 0.026^{*^{\wedge}}$
Conn.D	$90.591 \pm 3.717$	$70.486 \pm 11.811^*$	$66.250 \pm 7.714^*$	$51.656 \pm 9.933^{*^{\wedge}}$
SMI	$0.915 \pm 0.473$	$1.476 \pm 0.387^*$	$1.615 \pm 0.272^*$	$2.007 \pm 0.332^{\#}$
Tb.N[mm]	$3.895 \pm 0.540$	$3.208 \pm 0.254^*$	$3.483 \pm 0.279^*$	$2.950 \pm 0.311^{*^{\wedge}}$
Tb.Sp[mm]	$0.253 \pm 0.040$	$0.310 \pm 0.028^*$	$0.282 \pm 0.031$	$0.339 \pm 0.037^{*^{\wedge}}$
Tb.Th[mm]	$0.060 \pm 0.008$	$0.052 \pm 0.004^*$	$0.054 \pm 0.003$	$0.049 \pm 0.005^*$
TMD[mgHA/ccm]	$173.73 \pm 52.970$	$116.377 \pm 25.825^*$	$131.092 \pm 18.021^*$	$91.865 \pm 15.445^{*^{\wedge}}$
BMD[mgHA/ccm]	$623.40 \pm 15.382$	$602.266 \pm 17.642$	$646.236 \pm 10.689^{\#}$	$611.278 \pm 24.086^{\wedge}$

Data are presented as means  $\pm$  SD. \* $P < 0.05$ , compared with SD + Sham group. # $P < 0.05$ , compared with SD + OVX group. ^ $P < 0.05$ , compared with KD + Sham group

**Fig. 1** Micro-CT 3D images and sectional views of the region of interest (ROI) from the L4 vertebrae



### Micro-FE analysis data

The micro-FE data showed the changes in the stress distribution among the groups. In the sectional view, we found that the stress distribution was focused on the cortical and cancellous bones in the SD + sham group, while the stress distribution was transferred mostly onto the cortical bone with the occurrence of osteoporosis in the SD + OVX, KD + sham and KD + OVX groups. But in the external view, the stress distribution was presented in the cortical bone, showing no significant differences among the groups (Fig. 2). The compression stiffness of the SD + Sham group, KD + Sham group, OVX + Sham group and KD + OVX group was  $2599.9 \pm 421.5$  N/mm,  $1964.3 \pm 182.33$  N/mm,  $1725.8 \pm 698.46$  N/mm and  $1668.6 \pm 204.37$  N/mm, respectively. The stiffness of the remaining three groups was lower than the SD + Sham group, but showed no significant difference among the three groups (Fig. 3).

### Correlation between microstructure and stiffness

Pearson correlation coefficient between stiffness and trabecular parameters (BV/TV, BMD, SMI, Tb.N, Tb.Th, and Tb.Sp) was 0.823, 0.829, -0.897, 0.672, 0.814 and -0.628, respectively.

The order of parameters that was positively correlated with stiffness was: BMD, BV/TV, Tb.Th and Tb.N, and negatively correlated are SMI and Tb.Sp (Fig. 4).

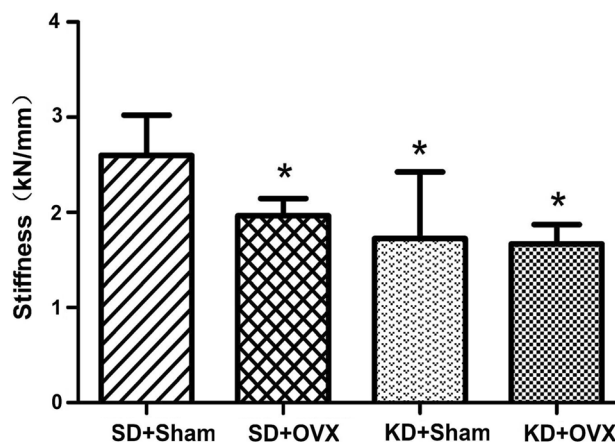


Fig. 3 Stiffness of compression test simulated by micro-FE of the L4 vertebrae. \* $P < 0.05$  compared to the SD + Sham group

### Vertebral compressive test results

The results of axial compression test showed that the Fmax in the SD + OVX ( $8.07 \pm 2.76$  N) and KD + OVX ( $7.92 \pm 3.21$  N) groups were remarkably decreased when compared with SD + Sham group ( $10.21 \pm 1.97$  N), ( $P = 0.048$  and  $P = 0.02$ ), but this trend was not observed in KD + Sham group (Fmax:  $10.46 \pm 1.78$  N,  $P = 0.798$ ). When compared with SD + OVX group, the Fmax in KD + Sham group was obviously higher ( $P = 0.019$ ) and there were no significant differences between SD + OVX and KD + OVX groups (Fig. 5).

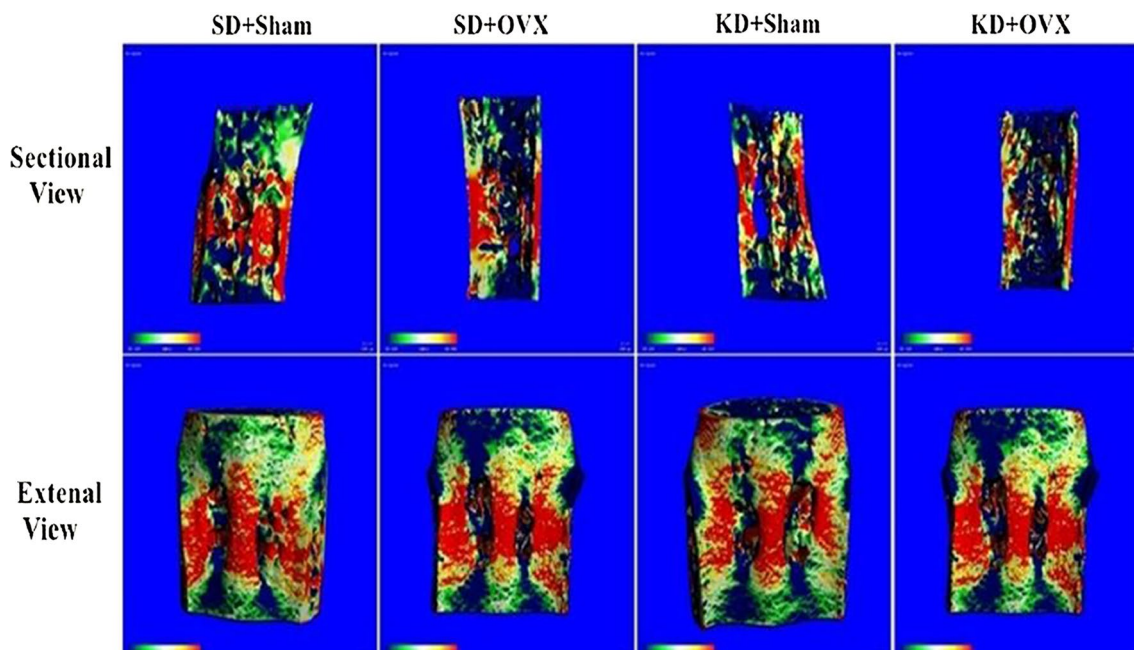


Fig. 2 Stress distribution diagrams of the L4 vertebrae after compression test simulated by FE

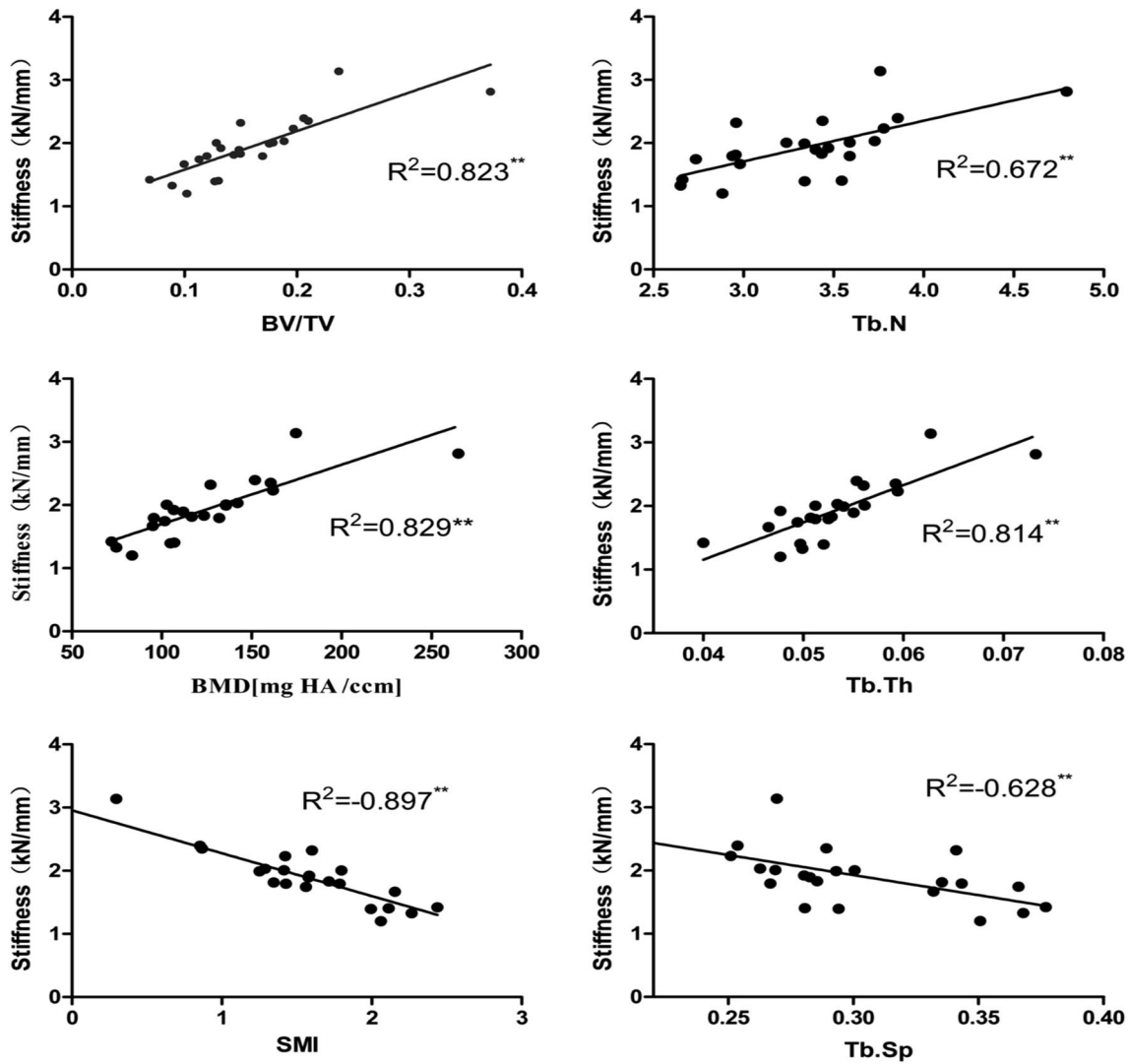


Fig. 4 The scatter diagram and best-fit line between microstructure parameters and stiffness (\* $p < 0.05$ , \*\* $P < 0.01$ )

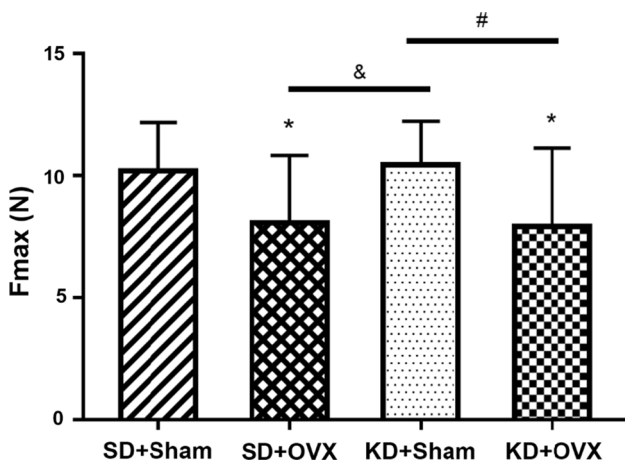


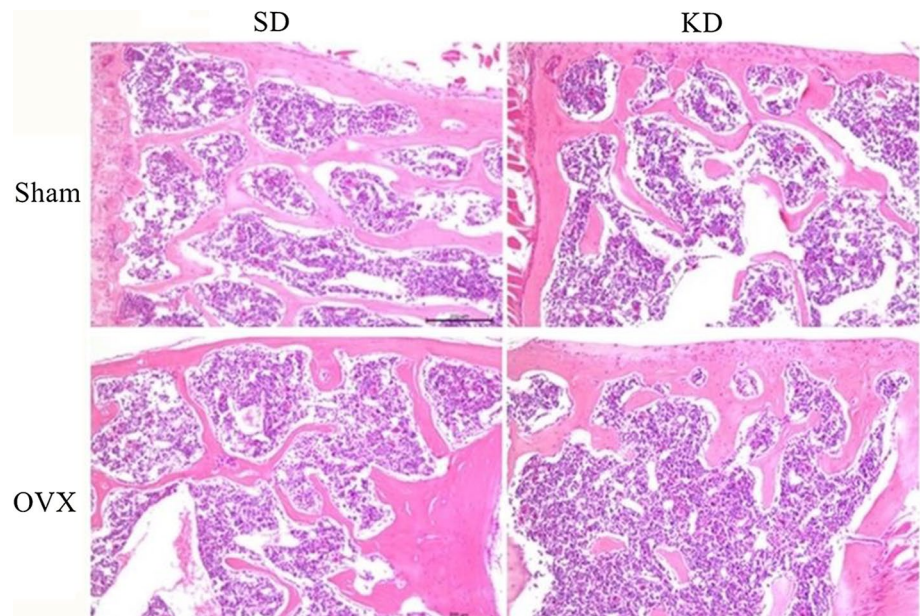
Fig. 5 Failure load of L4 vertebrae compression test in mice. \* $P < 0.05$ , compared with SD+Sham group. # $P < 0.05$ , compared with SD+OVX group. ^ $P < 0.05$ , compared with KD+Sham group

### Histological evaluation

Hematoxylin–eosin staining showed that the number of trabeculae was obvious decreased, and breakage and loss of trabecular bone in both OVX + Sham and KD + Sham groups compared with SD + Sham group, while the cancellous bone destruction was more severe in the KD + OVX group in L5 vertebra when compared with the other three groups (Fig. 6).

### Discussion

The present study demonstrated that KD compromised the microstructure and mechanical properties of vertebra to a similar level as OVX did in mice. Vertebral body is composed of internal cancellous bone and a thin coating of cortical bone. Cancellous bone of vertebral body is crucial

**Fig. 6** The hematoxylin–eosin staining of L5 vertebrae

for the function of the whole spinal column [21]. Although, the underlying probabilistic distributions of size, orientation, and spatial arrangement of individual trabeculae are statistically similar in different age, sex, anatomic location, and bone volume fraction [22], trabecular bone mass of vertebra is much lower than that of the peripheral bone [23]. The combination of KD with OVX may lead to more severe bone loss, but similar mechanical properties were observed with KD or OVX. Among parameters of cancellous bone, the BMD and BV/TV are both strongly correlated with the compressive stiffness, and the SMI was negatively correlated with the stiffness strongly. The current investigation extended our previous findings, indicating adverse effects of KD not only on the appendicular bone [18], but also on the axial bone of the mice.

To our knowledge, the effects of KD on vertebral body microstructures and mechanical properties were seldom studied in animal models. To evaluate the osteoporotic effects of KD, we included ovariectomized mice model as a positive control, and the combination of KD with OVX was used to explore if they have synergistic effects on bone loss. Besides, it could also compare the characteristics of KD and OVX on vertebral bony changes. Postmenopausal osteoporosis is a skeletal disease characterized by reduction of bone mass and enhanced bone resorption induced by estrogen deficiency [24]. The OVX animal model is widely used to simulate osteoporosis and reflect the trabecular bone changes in postmenopausal women especially [25, 26]. The successful establishment of ovariectomized mice model was confirmed by significant reduction of uterus weight in ovariectomized mice, which was consistent with the previous study findings [27]. Many literature studies reported that ovariectomized rats showed significantly impaired bone

mass and bone structure [28, 29], and even in lumbar vertebrae of the mice [30].

Dual-energy X-ray absorptiometry (DEXA) is the most common method to diagnose osteoporosis clinically. However, this technique can only predict 40–70% of vertebral fractures as it can only measure the areal BMD, which does not account for 3D geometry and BMD distribution [31]. In our previous study [18], we revealed that the BMD and BV/TV of the cancellous bone in femur were declined significantly in the KD + Sham and the SD + OVX groups, but these parameters showed no observable differences between KD + Sham and the SD + OVX groups, which was similar to the findings of L4 in the present study. Meanwhile, KD combined with OVX resulted in most severe micro-architectural changes on the cancellous bone of L4, which were also in accordance with the results on femur in our previous study [18]. Thus, it can be inferred that KD may compromise the microstructure of both lumbar vertebra and long bone in mice, and KD combined with OVX may lead to more loss of the cancellous bone. This was because the low BMD-induced compression fractures are the most common type of osteoporotic vertebral fractures observed in older adults [20].

In addition to the microstructure characteristics, biomechanical property is also an important index for studying osteoporosis, in which stiffness is one of the most important parameters that reflect the abilities of an object to resist breaking [20]. Therefore, to verify that the KD compromises vertebral biomechanics, the biomechanical tests of lumbar vertebra are very important. The axial compression test is a main biomechanical test that was applied to estimate the properties of cancellous bone [13]. In the present study, the axial compression stiffness was investigated by micro-finite

element simulation test. The linear micro-FE models using images at resolutions of  $\sim 80 \mu\text{m}$  and less than that can offer a promising method for examining the microarchitecture-related bone quality effects associated with aging, disease, and treatment [32] of humerus, femur and vertebrae [33, 34]. Micro-FE was validated to assess the mechanical properties of bone at the tissue scale [35], including the individual properties of the trabecular bone and cortical bone, and it can provide an accurate and stable estimates of bone strength [36, 37], thus considered as a preferable choice under this circumstance.

The present study simulated a compression test on the full vertebral body after ‘cutting off’ the endplates in micro-CT constructed 3D models, and obtained the stiffness of the L4 vertebra. The results showed that the mechanical property of the L4 was reduced in SD + OVX group when compared with that of the SD + Sham group, which was consistent with the classical compression test [29]. Severe trabecular bone loss was observed in mice under either KD or OVX intervene, leading to a declination in biomechanical properties. The micro-FE analysis indicated that KD, OVX, and the combination of KD with OVX might reduce the mechanical property of the L4, but showed no differences among them. The compression test of vertebra focused not only on cancellous, but also on cortical bone. Thus, the KD + Sham and SD + OVX groups displayed similar stiffness as they both induced same level of cancellous bone loss. The stiffness was not aggravated in the KD + OVX group, even though it had the most deteriorated cancellous bone structure. This was probably because it was not that severe to reflect on the mechanical properties of cortical bone [18]. To recognize the relationship of the microstructure and the mechanical properties of the vertebral body, we analyzed the correlation between the structural parameters and stiffness. The mechanical properties significantly depend on the apparent density of the bone, and this view was applied to porous materials [20, 38]. There is an obvious dependence of the properties on the architecture of trabecular bone as cancellous bone is inherently anisotropic. In our previous study of ovariectomized rats, the strength of the vertebrae depended mainly on the cortical component rather than deteriorated trabecular microstructure [39]. However, the present study showed that the stiffness also had a significant relationship with the microstructure parameters of cancellous bone. The BV/TV, BMD and Tb.Th were positively correlated with stiffness, while SMI or Tb.Sp was negatively correlated. This may provide a guideline for future studies regarding the relationship between cancellous microstructure and biomechanical change in bone diseases.

Although micro-FE validated the mechanical properties of bone at the tissue scale [35], direct biomechanical testing of bone undoubtedly provides more information about mechanical integrity [40]. The bone strength of the axial

skeleton was evaluated using a compression test to observe the changes of mechanical properties in osteoporosis or its prevention and treatment. In the present study, we performed the vertebral compressive test by a materials testing machine to observe the biomechanical property of L4 vertebra. The results showed that  $F_{\text{max}}$  was reduced significantly in the OVX + SD group compared with SD + Sham group, but showed no difference between SD + Sham and KD + Sham groups. Meanwhile, the KD + OVX group exhibited similar level of  $F_{\text{max}}$  as OVX + SD group did. The biomechanical behaviors from micro-FE and the compressive test were inconsistent. This could be due to that the vertebral samples were too small to perform the compressive test and the cranial and caudal sides of the vertebrae were irregular, which required removal of upper and lower endplates before test. But undeniably, the limited sample was also one of our study limitations.

## Limitations

The first limitation of this study was that we did not explore the mechanisms of KD-related osteoporosis, even if found KD might occur due to the promotion of bone absorption via activating osteoclasts rather than due to the inhibition of bone formation mediated by osteoblasts in mice [18]. The KD used in the experiment contains less mineral supply compared to SD, which means that osteomalacia due to solar vitamin D and/or dietary calcium deficiency may be the reason for bone loss in vertebrae. The follow-up studies will avoid differences in the mineral content of the two diets, leading to more definitive results. Besides, the content of calcium, phosphorus and vitamin D in the ketogenic fodder that we used was lower than SD. Although KD may still lead to bone loss even with adequate supply of calcium, phosphate and vitamin D [41], further studies should be conducted based on the same mineral and vitamin content to make the conclusion more persuasive. Moreover, although the vertebral bone is mainly composed of cancellous bone, further analysis of cortical bone changes caused by KD can make the experiment more comprehensive. Finally, the mice chosen in this study were young, thus the influence of KD on mature mice should be further studied.

## Conclusion

The present research demonstrated that long-term KD regimen might lead to decreased bone mass, bone quality and mechanical properties in mice vertebrae, and whose integrated effects were similar to OVX mice. Moreover, there was a strong correlation coefficient between BV/TV, BMD, Tb.Th and SMI with stiffness, which may in turn provide

a guideline for future studies on the relationship between microstructure and biomechanical changes in bone diseases.

## Compliance with ethical standards

**Conflict of interest** All authors declare that they have no conflict of interest.

## References

- Kose E, Guzel O, Demir K, Arslan N (2017) Changes of thyroid hormonal status in patients receiving ketogenic diet due to intractable epilepsy. *J Pediatr Endocrinol Metab* 30:411–416
- McArtney R, Bailey A, Champion H (2016) What is a ketogenic diet and how does it affect the use of medicines? *Arch Dis Child Educ Pract Ed* 102:194–199
- Branco AF, Ferreira A, Simoes RF, Magalhaes-Novais S, Zehowski C, Cope E, Silva AM, Pereira D, Sarda VA, Cunha-Oliveira T (2016) Ketogenic diets: from cancer to mitochondrial diseases and beyond. *Eur J Clin Invest* 46:285–298
- Winesett SP, Bessone SK, Kossoff EH (2015) The ketogenic diet in pharmacoresistant childhood epilepsy. *Expert Rev Neurother* 15:621–628
- Van der Auwera I, Wera S, Van Leuven F, Henderson ST (2005) A ketogenic diet reduces amyloid beta 40 and 42 in a mouse model of Alzheimer's disease. *Nutr Metab (Lond)* 2:28
- Prins ML, Fujima LS, Hovda DA (2005) Age-dependent reduction of cortical contusion volume by ketones after traumatic brain injury. *J Neurosci Res* 82:413–420
- Tai KK, Nguyen N, Pham L, Truong DD (2008) Ketogenic diet prevents cardiac arrest-induced cerebral ischemic neurodegeneration. *J Neural Transm (Vienna)* 115:1011–1017
- Tai KK, Truong DD (2007) Ketogenic diet prevents seizure and reduces myoclonic jerks in rats with cardiac arrest-induced cerebral hypoxia. *Neurosci Lett* 425:34–38
- Puchowicz MA, Zechel JL, Valerio J, Emancipator DS, Xu K, Pundik S, LaManna JC, Lust WD (2008) Neuroprotection in diet-induced ketotic rat brain after focal ischemia. *J Cereb Blood Flow Metab* 28:1907–1916
- Hahn TJ, Halstead LR, DeVivo DC (1979) Disordered mineral metabolism produced by ketogenic diet therapy. *Calcif Tissue Int* 28:17–22
- Bergqvist AG, Schall JI, Stallings VA (2007) Vitamin D status in children with intractable epilepsy, and impact of the ketogenic diet. *EPILEPSIA* 48:66–71
- Bergqvist AC, Schall JI, Stallings VA, Zemel BS (2008) Progressive bone mineral content loss in children with intractable epilepsy treated with the ketogenic diet. *Am J Clin Nutr* 88:1678–1684
- Chen B, Li Y, Yang X, Xie D (2012) Femoral metaphysis bending test of rat: introduction and validation of a novel biomechanical testing protocol for osteoporosis. *J Orthop SCI* 17:70–76
- Rachner TD, Khosla S, Hofbauer LC (2011) Osteoporosis: now and the future. *Lancet* 377:1276–1287
- Lane NE (2006) Epidemiology, etiology, and diagnosis of osteoporosis. *Am J Obstet Gynecol* 194:S3–S11
- Verhulp E, van Rietbergen B, Muller R, Huiskes R (2008) Indirect determination of trabecular bone effective tissue failure properties using micro-finite element simulations. *J Biomech* 41:1479–1485
- Johnell O, Kanis JA (2006) An estimate of the worldwide prevalence and disability associated with osteoporotic fractures. *Osteoporos Int* 17:1726–1733
- Wu X, Huang Z, Wang X, Fu Z, Liu J, Huang Z, Kong G, Xu X, Ding J, Zhu Q (2017) Ketogenic diet compromises both cancellous and cortical bone mass in mice. *Calcif Tissue Int* 101:412–421
- Wu J, Moverare-Skrtic S, Borjesson AE, Lagerquist MK, Sjogren K, Windahl SH, Koskela A, Grahemo L, Islander U, Wilhelmson AS, Tivesten A, Tuukkanen J, Ohlsson C (2016) Enzalutamide reduces the bone mass in the axial but not the appendicular skeleton in male mice. *Endocrinology* 157:969–977
- Muller R, Ruegsegger P (1995) Three-dimensional finite element modelling of non-invasively assessed trabecular bone structures. *Med Eng Phys* 17:126–133
- Ruyssen-Witrand A, Gossec L, Kolta S, Dougados M, Roux C (2007) Vertebral dimensions as risk factor of vertebral fracture in osteoporotic patients: a systematic literature review. *Osteoporos Int* 18:1271–1278
- Zhao F, Kirby M, Roy A, Hu Y, Guo XE, Wang X (2018) Commonality in the microarchitecture of trabecular bone: a preliminary study. *Bone* 111:59–70
- Chen H, Kubo KY (2014) Bone three-dimensional microstructural features of the common osteoporotic fracture sites. *World J Orthop* 5:486–495
- Boyd SK, Davison P, Muller R, Gasser JA (2006) Monitoring individual morphological changes over time in ovariectomized rats by in vivo micro-computed tomography. *Bone* 39:854–862
- Genant HK, Baylink DJ, Gallagher JC (1989) Estrogens in the prevention of osteoporosis in postmenopausal women. *Am J Obstet Gynecol* 161:1842–1846
- Li L, Chen X, Lv S, Dong M, Zhang L, Tu J, Yang J, Zhang L, Song Y, Xu L, Zou J (2014) Influence of exercise on bone remodeling-related hormones and cytokines in ovariectomized rats: a model of postmenopausal osteoporosis. *PLoS One* 9:e112845
- Zaid SS, Sulaiman SA, Sirajudeen KN, Othman NH (2010) The effects of Tualang honey on female reproductive organs, tibia bone and hormonal profile in ovariectomized rats—animal model for menopause. *BMC Complement Altern Med* 10:82
- Campbell GM, Buie HR, Boyd SK (2008) Signs of irreversible architectural changes occur early in the development of experimental osteoporosis as assessed by in vivo micro-CT. *Osteoporos Int* 19:1409–1419
- Hsu PY, Tsai MT, Wang SP, Chen YJ, Wu J, Hsu JT (2016) Cortical bone morphological and trabecular bone microarchitectural changes in the mandible and femoral neck of ovariectomized rats. *PLoS One* 11:e154367
- Lei T, Liang Z, Li F, Tang C, Xie K, Wang P, Dong X, Shan S, Jiang M, Xu Q, Luo E, Shen G (2018) Pulsed electromagnetic fields (PEMF) attenuate changes in vertebral bone mass, architecture and strength in ovariectomized mice. *Bone* 108:10–19
- Sornay-Rendu E, Munoz F, Garnero P, Duboeuf F, Delmas PD (2005) Identification of osteopenic women at high risk of fracture: the OFELY study. *J Bone Miner Res* 20:1813–1819
- Bevill G, Keaveny TM (2009) Trabecular bone strength predictions using finite element analysis of micro-scale images at limited spatial resolution. *Bone* 44:579–584
- Ladd AJ, Kinney JH, Haupt DL, Goldstein SA (1998) Finite-element modeling of trabecular bone: comparison with mechanical testing and determination of tissue modulus. *J Orthop Res* 16:622–628
- Kabel J, van Rietbergen B, Dalstra M, Odgaard A, Huiskes R (1999) The role of an effective isotropic tissue modulus in the elastic properties of cancellous bone. *J Biomech* 32:673–680

35. Tsafnat N, Wroë S (2011) An experimentally validated micro-mechanical model of a rat vertebra under compressive loading. *J Anat* 218:40–46
36. Arias-Moreno AJ, Ito K, van Rietbergen B (2016) Micro-Finite Element analysis will overestimate the compressive stiffness of fractured cancellous bone. *J Biomech* 49:2613–2618
37. Torcasio A, Zhang X, Duyck J, van Lenthe GH (2012) 3D characterization of bone strains in the rat tibia loading model. *Biomech Model Mechanobiol* 11:403–410
38. Gibson LJ (1985) The mechanical behaviour of cancellous bone. *J Biomech* 18:317–328
39. Ito M, Nishida A, Koga A, Ikeda S, Shiraishi A, Uetani M, Hayashi K, Nakamura T (2002) Contribution of trabecular and cortical components to the mechanical properties of bone and their regulating parameters. *Bone* 31:351–358
40. Liu Q, Xu X, Yang Z, Liu Y, Wu X, Huang Z, Liu J, Huang Z, Kong G, Ding J, Li R, Lin J, Zhu Q (2019) Metformin alleviates the bone loss induced by ketogenic diet: an in vivo study in mice. *Calcif Tissue Int* 104:59–69
41. Bielohuby M, Matsuura M, Herbach N, Kienzle E, Slawik M, Hoeflich A, Bidlingmaier M (2010) Short-term exposure to low-carbohydrate, high-fat diets induces low bone mineral density and reduces bone formation in rats. *J Bone Miner Res* 25:275–284

**Publisher's Note** Springer Nature remains neutral with regard to jurisdictional claims in published maps and institutional affiliations.